Semiconductor Physics, Quantum Electronics & Optoelectronics, 2022. V. 25, No 3. P. 331-341.

Optoelectronics and optoelectronic devices

Experimental investigation and theoretical modeling of textured silicon solar cells with rear metallization

A.V. Sachenko[1*], V.P. Kostylyov[1], R.M. Korkishko[1], V.M. Vlasiuk[1*], I.O. Sokolovskyi[1], M. Evstigneev[2], O.Ya. Olikh[3], A.I. Shkrebtii[4], B.F. Dvernikov[1], V.V. Chernenko[1]

[1]*V. Lashkaryov Institute of Semiconductor Physics, NAS of Ukraine, 03680 Kyiv, Ukraine*
[2]*Department of Physics and Physical Oceanography, Memorial University of Newfoundland, St. John's, NL, A1B 3X7, Canada*
[3]*Taras Shevchenko National University of Kyiv, 01601 Kyiv, Ukraine*
[4]*Ontario Tech University, Oshawa, ON, L1G 0C5, Canada*
[*]*Corresponding authors: viktorvlasiuk@gmail.com, avsacenko@gmail.com*

Abstract. Crystalline Silicon (c-Si) remains a dominant photovoltaic material in solar cell industry. Currently, scientific and technological advances enable producing the c-Si solar cells (SCs) efficiency close to the fundamental limit. Therefore, combining the experimental results and those of modeling becomes crucial to further progress in improving the efficiency and reducing the cost of photovoltaic systems. We carried out the experimental characterization of the highly-efficient c-Si SCs and compared with the results of modeling. For this purpose, we developed and applied to the samples under investigation the improved theoretical model to optimize characteristics of highly efficient textured solar cells. The model accounts for all recombination mechanisms, including nonradiative exciton recombination by the Auger mechanism *via* a deep recombination centers and recombination in the space-charge region. To compare the theoretical results with those of experiments, we proposed empirical formula for the external quantum efficiency (*EQE*), which describes its experimental spectral dependence near the long-wave absorption edge. The proposed approach allows modeling of the short-circuit current and photoconversion efficiency in the textured crystalline silicon solar cells. It has been ascertained that the dependences of the short-circuit current on the open-circuit voltage and the dark current on the applied voltage at $V < 0.6$ V coincide with each other. The theoretical results, as compared to the experimental ones, allowed us to validate the developed formalism, and were used to optimize the key parameters of SCs, such as the base thickness, doping level and others. In this work, we have further generalized and refined the analytical approach proposed and used by us earlier to analyze high-efficiency solar cells and model their characteristics.

Keywords: silicon, solar cell, texture, efficiency, recombination, optimization.

https://doi.org/10.15407/spqeo25.03.331
PACS 88.40.hj, 88.40.jj

Manuscript received 05.07.22; revised version received 30.08.22; accepted for publication 21.09.22; published online 06.10.22.

1. Introduction

Today, solar panels, made using polycrystalline and crystalline silicon, dominate the photovoltaic market, contributing to more than 90% of the global solar energy production [1, 2]. The current efficiency record of c-Si solar cells (SCs) is 26.7% [3, 4] against an intrinsic limit of 29.7% [5]. The efforts of scientists and engineers in the field, on the one hand, are aimed at further enhancing the efficiency of SCs photoconversion, and, on the other hand, at reducing a cost of solar panels. High-performance crystalline silicon-based solar cells with the efficiency of 20% and above are based on *p*-*n* junctions or heterojunctions with very thin layers of amorphous hydrogenated silicon SCs [3, 4, 6]. These SCs have several features in common: first, their tops or both top and bottom surfaces are textured, which significantly reduces reflection of the incident light and enhances the light trapping. To increase the SCs energy output by maximizing their photoconversion efficiency η, surface texturing techniques are developed to reduce the optical reflection losses and maximize the light absorbed. Therefore, surface texturing of silicon photovoltaic systems currently is drawing much attention [2, 6, 7]. The

© 2022, V. Lashkaryov Institute of Semiconductor Physics, National Academy of Sciences of Ukraine

second common feature is that the Shockley–Reed–Hall (SRH) lifetime, responsible for the recombination in the bulk, is several milliseconds and the diffusion length of excess charge carriers is much longer than SC thickness. Currently, further increase of the silicon SC efficiency becomes more and more difficult, and requires better consideration of the physical processes in SCs. In particular, to further increase the SC efficiency, it is necessary to take into account all contributing recombination mechanisms in silicon. This has to include a non-radiative exciton recombination by the Auger mechanism *via* deep impurity centers [8] and recombination in the space charge region (SCR) [9]. Still, the above two mechanisms are not included in the existing SC optimization formalisms and software [10]. However, as we previously demonstrated [11], these recombination processes are detrimental in the high-efficiency silicon-based SCs. They can significantly influence the SCs efficiency, as compared to the mechanisms that are already considered, in particular, the radiative and band-to-band Auger recombinations.

Particularly challenging are calculations of the absorption and external quantum efficiency of textured silicon SCs. Even though the existing optimization software packages are advanced enough, they do not provide the unique solution of the problem of the thickness optimization for textured SCs. However, in one of our papers [12] we offered a solution of the problem by introducing a simple empirical formula for calculating the external quantum efficiency, which allows one to successfully solve the problems with the absorption and external quantum efficiency, of which the available formalisms suffer.

Therefore, to advance in improvement of the SCs efficiency, the available optimization approaches should be further developed and applied to highly efficient SCs, which is the goal of this work. To model and optimize the textured high-efficiency silicon SCs, we first measured and analyzed the experimental dependences of the external quantum efficiency (*EQE*). Next, we calculated the short-circuit current and the photoconversion efficiency under AM1.5 conditions, which are dependent on the SC base thickness *d* and its doping level. The results were applied to optimize characteristics of the textured silicon SCs by using the concept of a completely randomized Lambert surface [13], which is the commonly accepted model for surface texturing from the reflection reduction viewpoint. However, we stress that the presented theoretical approach is applicable to any arbitrary textured SCs surface and all the main types of silicon-based high efficiency textured SCs.

The presented self-consistent approach for the textured Si solar cell efficiency η has been validated experimentally. Dark and light *I–V* characteristics as well as the light intensity dependence of open-circuit voltage were measured for a number of highly efficient silicon *p-n* junction SCs with the photoconversion efficiency $\eta \geq 20\%$. The important component of the formalism, namely spectral dependences of *EQE*(λ) under AM1.5 conditions were also investigated experimentally.

For the textured silicon SCs considered, the experimental dependences of *EQE*(λ) were analyzed. It has been shown that close to the long-wave absorption edge *EQE*(λ) dependence can be accurately described by the empirical formula with a variable parameter dependent on SC. Using the experimental *EQE*(λ) dependence represented by the proposed formula, we calculated the dependence of the short-circuit current density J_{SC} on the base thickness *d* for textured SCs.

In the calculations and comparison of the theory with the experiment, in addition to the radiative and Auger recombinations, we also considered nonradiative exciton recombination by the Auger mechanism *via* deep recombination centers [14] and recombination in SCR [15]. This work generalizes and refines the analytical approach that we used earlier to analyze high-efficiency solar cells and to model their characteristics.

The paper is organized as follows. We describe first in the section 2 the experimental details and the recombination mechanisms in the considered silicon-based SCs. In the section 3, we offer the description of optimization formalism. Experimental results, as compared to the simulations, will be presented in the section 4. The section 5 offers the summary of the research.

2. Technical details and main parameters

Dark current-voltage (*I–V*) characteristics were measured using the samples of high-efficiency SCs ($\eta \geq 20\%$) with an external source of direct voltage. The short-circuit current density J_{sc} dependence on the open-circuit voltage V_{OC} was measured within a wide incoming irradiance range of 10…1200 W/m^2 by using a set of attenuating filters. Light *I–V* characteristics were measured under the AM1.5G conditions (1000 W/m^2) at 25 °C.

The spectral dependences of external quantum efficiency *EQE*(λ) were measured using the SCs short-circuit mode within the wavelength range Δλ of 360…1200 nm with the grating monochromator, automatically maintaining the constant flux of monochromatic photons at a specified level. To reach this, the photon flux was divided using the oscillating beam splitter with the frequency 20 Hz by the channel for maintaining the photon flux at a given constant level and the channel for measuring the external quantum efficiency of the sample under investigation. In this case, the photon flux was modulated with the frequency 20 Hz. Amplification of the alternating signal with this frequency followed by a lock-in amplifier with an improved signal-to-noise ratio.

All the experimental measurements were performed using the equipment of Solar Cell and Photovoltaic Panel Testing Center of the ISP NAS of Ukraine, which is the only measuring laboratory in Ukraine certified for technical competence and independence by authorized state bodies in accordance with the Law of Ukraine "On metrology and metrological activity" for performing the tests of SCs and solar panels. The center is equipped with the following installation and standard samples:

Solar Simulator; Reference PV Cells; Installation for testing the photoelectrical parameters of solar cells; Installation for measuring the spectral characteristics of photoconverters, Software to automate testing and the others.

To demonstrate application of the formalism by comparing the experimental results and the theoretical ones, we characterize experimentally the back junction back contact solar cells, also called as interdigitated back contact solar cells (IBC SCs)). In particular, we measured characteristics of the commercial textured silicon *p-n* junction SCs with a photoconversion efficiency η above 21%, which are manufactured by SunPower™.

For the modeling and optimization of the photo-conversion efficiency inherent to SCs in terms of base thickness *d* and the doping level *n*, we used the analytical expression for *EQE*(λ). We ascertained that the experimental spectral dependences of external quantum efficiency *EQE*(λ) in the textured silicon SCs near the long-wave absorption edge can be described by the empirical formula $EQE(\lambda)=\left[1+b/\left(4n_r(\lambda)^2\alpha(\lambda)d\right)\right]^{-1}$,

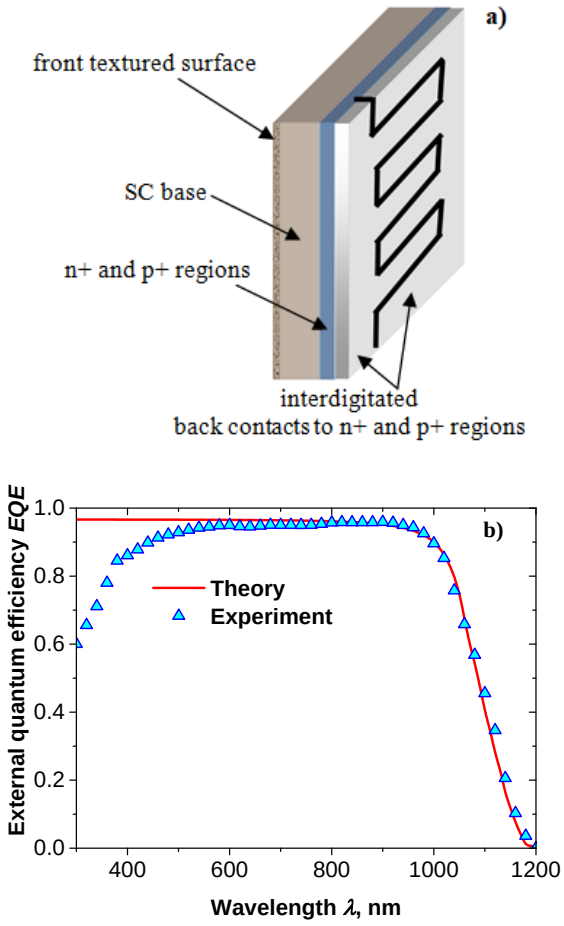

Fig. 1. Sketch of the interdigitated back contact solar cell investigated and modeled in this work (a). Experimental (triangles) and theoretical (calculated using the empirical formula, red line) dependences of *EQE*(λ) for SunPower™ IBC SC under investigation (b).

where α(λ) is the light absorption coefficient, *d* is the base thickness, n_r is the refractive index, and *b* is a non-dimensional coefficient that characterizes texturing quality and ranges from 1.6 to 4. It is usually higher than unity, when *b* = 1 the above empirical formula transforms into the well-known Yablonovitch formula [16] for absorbance. Physical meaning of the parameter *b* is the ratio of the photon path length in the case of a perfectly randomized surface, considered in [13], to the photon path length in a particular sample with an imperfectly randomized surface.

Fig. 1 shows a sketch of SC (a) and experimental external quantum efficiency *EQE*(λ), measured for the investigated SunPower™ IBC SC (b), as compared to that from the empirical formula, the parameter *b* = 4 was used.

The minority carrier lifetime τ is one of the most important parameters for characterization of semiconductor, which is used in SCs [17]. The total effective recombination time τ_{eff}, which includes all recombination mechanisms, can be written as:

$$\tau_{eff}(n)=\left[\begin{array}{l}\dfrac{1}{\tau_{\mathrm{SRH}}(n)}+\dfrac{1}{\tau_{nr}(n)}+\dfrac{S_{0S}}{d}\left(1+\dfrac{\Delta n}{n_0}\right)+\\ +\dfrac{1}{\tau_r(n)}+\dfrac{1}{\tau_{\mathrm{Auger}}(n)}+\dfrac{S_{SC}(n)}{d}\end{array}\right]^{-1}, \qquad (1)$$

where $n=n_0+\Delta n$ is the total concentration of the majority carries (electrons, for definiteness) with the equilibrium concentration, n_0 is the base doping level and Δn is the excess concentration of electron-hole pairs (EHPs). $S_{0S}=S_{00}+S_{0d}$ is the total surface recombination velocity at the front and back surfaces of the solar cell in the low-injection regime, $\tau_r(n)=\tau_{\mathrm{SRH}}\cdot(n_x/n)$ is the nonradiative exciton recombination time [8], $n_x=8.2\cdot10^{15}$ cm^{-3}, $\tau_r(n)$ is the radiative recombination time [4], $\tau_{\mathrm{Auger}}(n)$ is the Auger interband recombination time [18], and S_{SC} is the recombination rate in SCR.

The Shockley–Read–Hall recombination time τ_{SRH} for *n*-type Si can be written as:

$$\tau_{\mathrm{SRH}}(n)\cong\frac{\tau_{p0}(n_0+\Delta n+n_1)+\tau_{n0}(p_1+\Delta n)}{n_0+\Delta n}, \qquad (2)$$

where $\tau_{p0}=(C_pN_t)^{-1}$ s and $\tau_{n0}=(C_nN_t)^{-1}$ s, with the hole (electron) capture coefficient $C_p(C_n)$ by the recombination centers with the concentration N_t, while n_1 and p_1 denote the electron and hole densities, respectively, when the Fermi level coincides with the trap level, the so-called Shockley–Reed factors for electrons and holes.

Note that the Shockley–Reed–Hall lifetime τ_{SRH} depends on the recombination center location inside the gap and the capture coefficient for electrons and holes. With increasing the doping and excitation levels, the lifetime generally changes within the range between two values, and it can increase, decrease or remain practically constant. In what follows, we shall consider that τ_{SRH} is

constant in the standard range of the doping levels and excitation (for EHP, the excess concentration varies within the range from 10^{14} to 10^{16} cm^{-3}).

The expression for the radiative recombination lifetime can be written as [4]:

$$\tau_r^{-1} = B_r(1-P_{PR})(n_0+\Delta n), \quad (3)$$

where B_r is the radiative recombination parameter in silicon, and P_{PR} is the probability of photon reabsorption. Following [4], the expression for B_r is:

$$B_r = \int_0^\infty B(E)dE, \text{ with } B(E) = \left(\frac{n_r(E)\alpha(E)E}{\pi c\hbar^{3/2}n_i}\right)^2 e^{-\frac{E}{k_B T}}. \quad (4)$$

Here, $n_r(E)$ is the silicon refractive index, $\alpha(E)$ is the photon energy dependent absorption coefficient, and $E = hc/\lambda$.

The probability of photon reabsorption in the SC base can be defined as:

$$P_{PR} = B^{-1}\int_0^\infty A_{bb}(E)B(E)dE, \quad (5)$$

with the absorbance $A_{bb}(E)$ equals to

$$A_{bb}(E) = \frac{\alpha}{\alpha + b/4n_r^2 d}. \quad (6)$$

The expression (6) differs from that from [16], where it introduces a coefficient b higher than unity. As for the interband recombination lifetime $\tau_{\text{Auger}}(n)$, the empirical expression given in [18] is used.

The expression for the recombination rate in SCR S_{SC} is usually derived under the assumption that it occurs *via* a deep level, close to the middle of the band gap, and for the case of silicon it was presented and analyzed in [19, 20]. This was made within the model, when the discrete bulk deep level with the energy E_t is close to the middle of the band gap, with the concentration N_t^* and the capture cross-sections for electrons and holes σ_n and σ_p.

We used the following expression to calculate the recombination rate S_{nr} in SCR (see [9, 21]):

$$S_{SC}(\Delta n) = \int_0^w \frac{(n_0+\Delta n)dx}{\left[\left((n_0+\Delta n)e^{y(x)} + n_i(T)\exp\left(\frac{E_t}{kT}\right)\right) + b_r\left((p_0+\Delta n)e^{-y(x)} + n_i(T)\exp\left(-\frac{E_t}{kT}\right)\right)\cdot\tau_R\right]}. \quad (7)$$

Here, $b_r = C_p/C_n$, $C_n = V_{nT}\sigma_n$, $C_p = V_{pT}\sigma_p$, with the average thermal velocities of electrons and holes V_{nT} and V_{pT}, respectively, $\tau_R(x) = \left(C_p N_t^*(x)\right)^{-1}$ is the EHP lifetime in SCR, N_t^* is the deep level concentration in SCR, p_0 is the equilibrium bulk hole concentration, $y(x)$ is the dimensionless electrostatic potential in SCR, E_t is the energy of the deep level in silicon SCR, calculated from the middle of the gap, $n_i(T)$ is the concentration of intrinsic charge carriers, and w is the SCR thickness.

Moving from integration on the x coordinate to integration on the potential y, we obtain

$$S_{SC}(\Delta n) = \int_{y_w}^{y0} \frac{(n_0+\Delta n)dy}{\left[\left((n_0+\Delta n)e^{y} + n_i(T)\exp\left(\frac{E_t}{kT}\right)\right) + b_r\left((p_0+\Delta n)e^{-y} + n_i(T)\exp\left(-\frac{E_t}{kT}\right)\right)\tau_R\right]} F, \quad (8)$$

where

$$F = \frac{L_D}{\left[(1+\Delta n/n_0)(e^y-1) + y_m + \left(\frac{p_0}{n_0}+\Delta n/n_0\right)(e^{-y}-1)\right]^{1/2}} \quad (9)$$

Here, $L_D = \left(\varepsilon_0\varepsilon_{Si}kT/2q^2n_0\right)^{1/2}$ is the Debye length, q – elementary charge, y_0 – non-equilibrium dimensionless band bending on the surface of a weakly doped region, which depends on the level of excitation Δn and is defined by the equation of integral neutrality, y_w – non-equilibrium dimensionless potential at the boundary of SCR near the quasi-neutral region.

To find the dependence of the non-equilibrium dimensionless potential on the coordinate, it is necessary to use the solution of the Poisson equation (second integral), which has the following form:

$$x = \int_{y_0}^{y} \frac{L_D}{\left[\left(1+\frac{\Delta n}{n_0}\right)(e^{y_1}-1) - y_1 + \frac{\Delta n}{n_0}(e^{-y_1}-1)\right]^{0.5}} dy_1. \quad (10)$$

The value of the non-equilibrium dimensionless potential y_0 at $x = 0$ is determined from the solution of the equation of integral electroneutrality [19], which has the form

$$N = \pm\left(\frac{2kT\varepsilon_0\varepsilon_{Si}}{q^2}\right)^{1/2} \times \left[(n_0+\Delta n)(e^{y_0}-1) - n_0 y_0 + \Delta n(e^{-y_0}-1)\right]^{1/2}, \quad (11)$$

where qN is the surface charge density of acceptors in the *p-n* junction or in the anisotypic heterojunction.

In the analytical approximation for the recombination rate in SCR $S_{SC}^{a}(\Delta n)$, the following expression is valid:

$$S_{SC}^{a}(\Delta n) \approx \frac{kL_{\mathrm{D}}}{\tau_R} \frac{\exp(y_m)}{\left[(1+\Delta n/n_0)\left(e^{-y_m}-1\right)+y_m+\left(\frac{p_0}{n_0}+\Delta n/n_0\right)\left(e^{y_m}-1\right)\right]^{1/2}}, \quad (12)$$

where k is the numerical coefficient that is approximately equal to 2, and $y_m = (1/2)\ln\left((n_0+\Delta n)/b_r(p_0+\Delta n)\right)$.

It should be noted that the model of stepwise distribution of lifetime between the space charge region and the neutral bulk is too rough for calculations. It needs to be improved by taking into account the significant increase in SCR lifetime, since we approach neutral bulk, or use the Gaussian inverse distribution of lifetime values in SCR. Taking into account both one and the second factors allows one to use the results obtained using the expressions (8) and (9).

3. Photoconversion efficiency formalism

The light *I–V* characteristics for the solar cells (RC SCs) with rear contact metallization under consideration (IBC SCs)) were calculated using the expressions from [8, 18]:

$$I(V) = I_L - \frac{qA_{SC}d\Delta n}{\tau_{eff}(\Delta n)} - \frac{V+IR_S}{R_{sh}}, \quad (13)$$

$$I_r(V) = qA_{SC}\left(\frac{d}{\tau_{eff}^{b}} + S_{0S}\left(1+\frac{\Delta n}{n_0}\right)+\frac{A_B}{A_{AC}}S_{SC}\right)\Delta n(V), \quad (14)$$

$$\tau_{eff}^{b}(n) = \left[\frac{1}{\tau_{\mathrm{SRH}}(n)}+\frac{1}{\tau_r(n)}+\frac{1}{\tau_{rn}(n)}+\frac{1}{\tau_{\mathrm{Auger}}(n)}\right]^{-1}, \quad (15)$$

$$\Delta n(V) = -\frac{n_0}{2} + \sqrt{\frac{n_0^2}{4}+n_{i0}(T)^2 e^{\Delta E_g/kT}\left(\exp\left(\frac{q(V-IR_S)}{kT}-1\right)\right)}, \quad (16)$$

where $I(V)$ is the total current, I_L is the photogeneration current (note that at low values of series resistance R_S, which is always true for high-efficiency solar cells, $I_L \approx I_{SC}$ – short-circuit current), $I_r(V)$ is the recombination (dark) current, V is the applied voltage, $\tau_{eff}^{b}(n)$ is the effective bulk lifetime, R_S and R_{SH} are the series and shunt resistances, n_{i0} is the intrinsic concentration at low injection [22], and $\Delta E_g(n_0, \Delta n)$ is the magnitude of bandgap narrowing in Si [18].

The expression for the dark current in accord to (13) has the form:

$$I_D(V) = \frac{qA_{SC}d\Delta n}{\tau_{eff}(\Delta n)} + \frac{V-I_DR_S}{R_{sh}}. \quad (17)$$

The photogeneration current $I_L = I_{SC}$ dependence on the open-circuit voltage V_{OC} can be found from (13) by putting $I = 0$:

$$I_L = \frac{A_{SC}qd}{\tau_{eff}(\Delta n_{OC})}\Delta n_{OC} + \frac{V_{OC}}{R_{sh}} \quad (18)$$

with

$$\Delta n_{OC} = -\frac{n_0}{2} + \sqrt{\frac{n_0^2}{4}+n_{i0}^2 e^{\Delta E_g/kT}\left(\exp\left(\frac{qV_{OC}}{kT}-1\right)\right)}. \quad (19)$$

If we compare the expressions for Δn and Δn_{OC}, as well as for the dark current (17) and photogeneration current (18), it becomes obvious that they coincide, respectively, with each other, if we replace V by V_{OC} and I_D by I_L and also put R_S equal to zero in Eqs (16), (17).

This means that the solutions $I_D(V, R_{sh}, R_S)$ and $I_L(V_{OC}, R_{sh})$ are identical, if $R_S = 0$. And $V_{OC}(\Delta n_{OC})$ can be found from (19):

$$V_{OC} = \frac{kT}{q}\ln\left(\frac{(\Delta n_{OC}+n_0)\cdot\Delta n_{OC}}{n_{i0}(T)^2 e^{\Delta E_g/kT}}+1\right). \quad (20)$$

Multiplying the current $I(V)$ value on the applied voltage V, we get the SC generated power $P(V)$, and maximizing this by using $dP/dV = 0$ condition we find the voltage V_M at the point of maximum power. Substituting V_M into Eq. (13), we obtain the current I_M at the maximum power point. This allows calculating photoconversion efficiency η and the *I–V* fill-factor *FF* in the usual way. Note that in the used approximation, the short-circuit current I_{SC} value is a parameter that should be determined from the experimental data.

On the other hand, the short-circuit current in textured silicon SCs can be calculated, if the external quantum efficiency of the photocurrent $EQE(\lambda)$ is known. As it was shown in [12], for a number of high efficiency textured silicon SCs with *p-n* junctions and HIT elements, the external quantum yield in the long-wave region can be described using the following empirical formula:

$$EQE(\lambda) = \left(1+\frac{b}{4n(\lambda)^2\cdot\alpha(\lambda)d}\right)^{-1}, \quad (21)$$

where b is a numerical coefficient higher than unity. For SCs considered, both $EQE(\lambda)$, the experimental dependence and their approximation by using the expression (21) were adduced in Fig. 1. The value $b = 4$ leads to a good agreement of the experimental and calculated dependences in the important long-wave region within the range 800 up to 1200 nm. Using this

empirical formula for considered IBC SCs, the short-circuit current I_L at AM1.5 can be calculated using the formula:

$$I_L(d,b) = \\ = q\left[\int_{\lambda_0}^{800} I_{AM1,5}(\lambda)EQE(\lambda)d\lambda + f\int_{800}^{\lambda_m} I_{AM1,5}(\lambda)EQE(\lambda,b)d\lambda\right], \quad (22)$$

where λ_0 = 300 nm, λ_m = 1200 nm, $I_{AM1.5}(\lambda)$ is the spectral density of the photon flux at AM1.5, $EQE(\lambda, b)$ is defined by Eq. (21), and the coefficient $f \le 1$. The f value is chosen that at λ = 800 nm the values $EQE(\lambda, b)$ and $IQE(\lambda, b)$ coincide. In this way, the I_L dependence on the base thickness d can be found, which allows one to optimize SCs by choosing the base thickness.

4. Results and analysis

To validate the developed above theoretical approach and its application, we characterized experimentally the commercial textured silicon *p-n* junction SCs with a photoconversion efficiency η above 21%, which are manufactured by SunPower™ (Fig. 1a). SCs with rear contact metallization, have a photoactive area of 154.7 cm^2 and the base thickness d = 165 μm. Fig. 2 shows the experimental and theoretical dependences of $J_D(V)$ as well as $J_L(V_{OC})$ for SC at the temperature 25 °C.

The figure demonstrates that, when both V and V_{OC} are less than 0.62 V, the experimental $J_D(V)$ and $J_L(V_{OC})$ plots coincide. At high voltage values, the curves diverge because of influence of series resistance in the dark $J_D(V)$ dependences. This is consistent with the analysis above.

To theoretically model the dark J_D–V characteristics, it is necessary to find the recombination parameters, in particular τ_R and b_r, which defines the recombination rate in SCR. When modeling recombination in SCR, we used the expression (8).

The above theoretical result has been compared to the experimental dependence $J_D(V)$ that we have measured. The following parameters: $n_0 = 9\cdot10^{14}$ cm^{-3}, d = 165 μm, $\tau_m = 1.3\cdot10^{-5}$ s, b_r = 0.1, y_l = –0.1 were obtained from the fit: the total rate of surface recombination S_{0S} at a low excitation level is 5 cm/s. In this simulation, we assumed that τ_{SRH} = 10 ms, which is matched well with that from [23].

The theoretical $J_L(V_{OC})$ dependence can be found from a joint solution of Eqs (18) and (19) by using the same parameters as for calculation of the dark I–V characteristic. As can be seen from Fig. 2, there is a good agreement between the results of experiments and theory. In contrast to similar dependences reported in the literature (see, for example, [4, 6]), these both dependences were measured and calculated in a much wider range of J_L, including, in particular, the region of low photocurrent density J_L. Estimates show that at $J_L < 10^{-5}$A/cm^2 the inequality $V_{OC}/R_{sh} > J_L$ holds. In the case when $J_L = 4\cdot10^{-2}$ A/cm^2, as compared to that J_L, the value V_{OC}/R_{sh} is two and a half orders of magnitude less and can be neglected in Eq. (18).

Fig. 3 shows the theoretical dependences of $S_{SC}(\Delta n)$ and $S^a_{SC}(\Delta n)$, plotted using the expressions (2) – curve *1* and (12) – curve *2* and the above parameters, at which we achieve the best consistency between the experimental and theoretical results. As can be seen from Fig. 3, the dependences are represented by curves *1* and *2* (expressions (2) and (12), respectively) give quite similar results (in the calculations, the value of y_w was assumed to be –0.03). However, it should be noted that the expression (2) is exact, and the expression (12) is approximate. Therefore, when modeling one needs to use the expression (2).

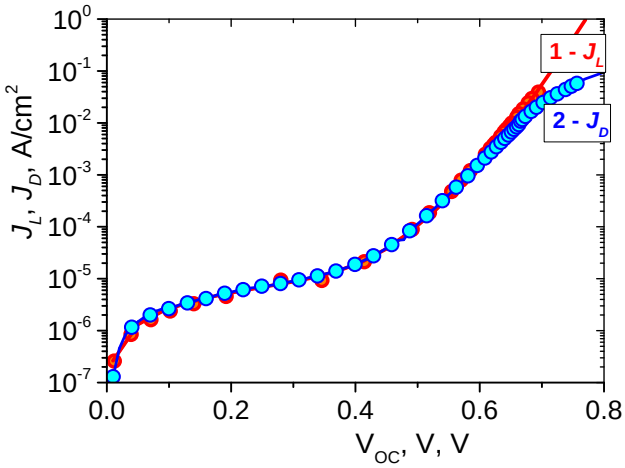

Fig. 2. Experimental dependences of the short-circuit current J_L on the open-circuit voltage V_{OC} (red points) and of dark current J_D on the applied voltage V (blue points). Lines are the theoretical dependences: *1* – $J_L(V_{OC})$, red line; *2* – $J_D(V)$, blue line.

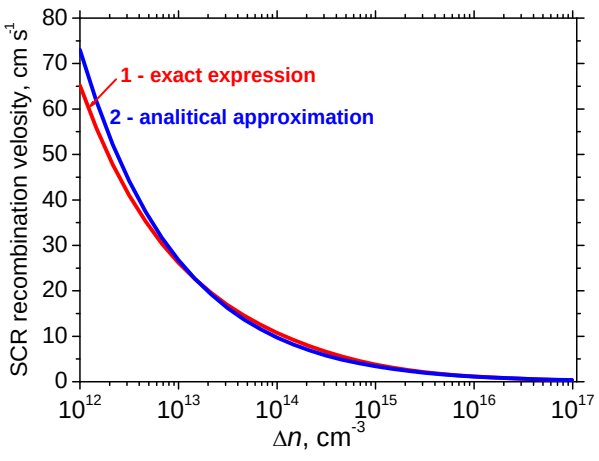

Fig. 3. Theoretical dependences of the recombination velocity in SCR on the excess concentration, $S_{SC}(\Delta n)$ (exact expression (2), curve *1*) and $S^a_{SC}(\Delta n)$ (analytical approximation (12), curve *2*).

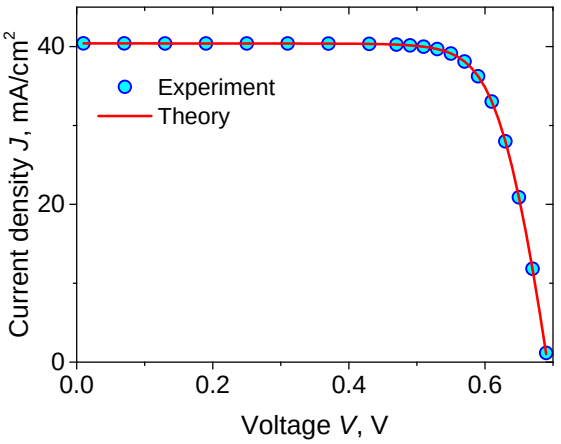

Fig. 4. Measured and calculated light *I–V* characteristics. Triangles are the experimental values; the solid line corresponds to the theoretical data.

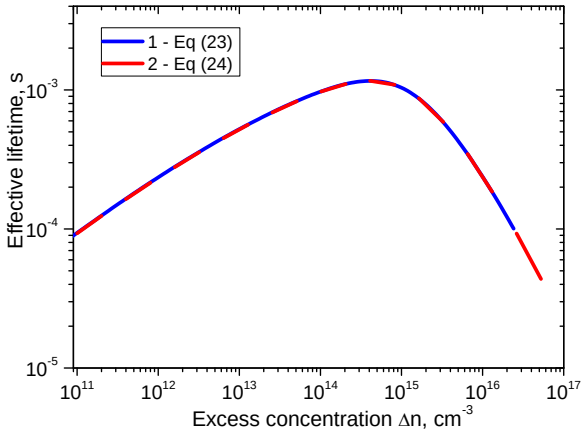

Fig. 5. Theoretical dependences $\tau_{eff}(\Delta n)$. Blue curve *1* is calculated using Eq. (23), while the red curve *2* is obtained using Eq. (24).

Fig. 4 shows the light *I–V* characteristic measured at AM1.5 for the SunPower™ SC with the open-circuit voltage V_{OC} = 0.692 V, and the short-circuit current density J_{SC} = 40.04 mA/cm^2. Experimental and calculated light *I–V* characteristics agree well, when using the same components of the effective lifetime as for the dark *I–V* characteristics.

We plot the $\tau_{eff}(\Delta n_{OC})$ dependence in Fig. 5 by using the expressions (23) and (24):

$$\tau_{eff\,1} = \frac{qd\Delta n_{OC}}{J_L - \dfrac{V_{OC}}{R_{sh}}}, \qquad (23)$$

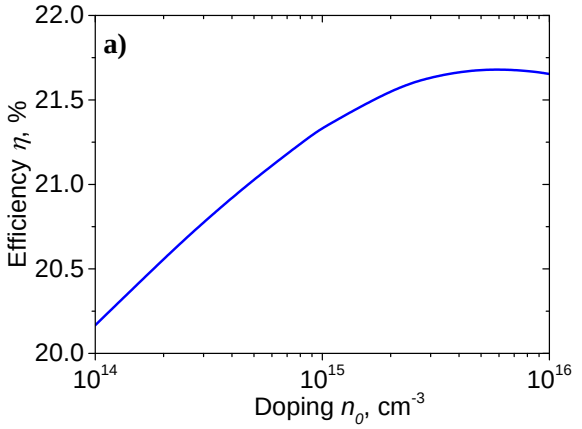

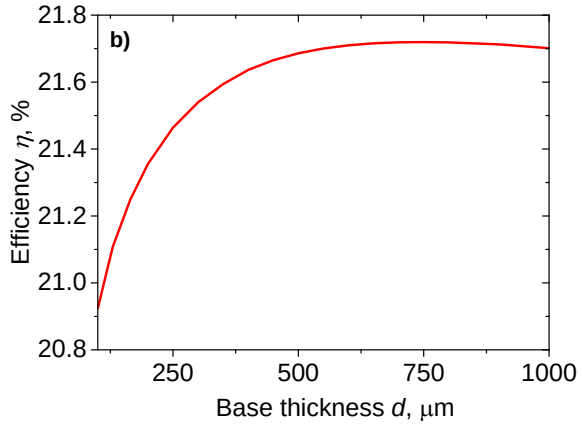

Fig. 6. Theoretical dependence of the photoconversion efficiency η on the base doping level n_0. Its maximum of 21.69% is achieved at $n_0 = 5.5\cdot10^{15}$ cm^{-3} (a). The photoconversion efficiency η dependence on the base thickness *d*. The efficiency maximum η = 21.72% is achieved at *d* = 750 μm (b).

As can be seen from the above dependences for τ_{eff1} and τ_{eff2}, they completely coincide with each other. This can be easily verified by carefully considering the equation (18).

The difference between dependences $\tau_{eff}(\Delta n)$ obtained from the expressions (23) and (24) is as follows. If the use of dependence (24) allows us to make it directly, substituting in the expression of dependence on Δn components of recombination, then when using (23) it happens indirectly. First, the value of the excess concentration of electron-hole pairs in the open-circuit mode and the open-circuit voltage are calculated, and then, using the expression for the short-circuit current, the dependence $\tau_{eff}(\Delta n)$ is found. But when calculating the equations to be solved, the dependences of recombination components on the excess concentration of electron-hole pairs are laid down.

$$\tau_{eff\,2} = \left[\frac{1}{\tau_{\mathrm{SRH}}(\Delta n_{OC})} + \frac{1}{\tau_r(\Delta n_{OC})} + \frac{1}{\tau_{nr}(\Delta n_{OC})} + \frac{1}{\tau_{\mathrm{Auger}}(\Delta n_{OC})} + \frac{S_{0S}}{d}\left(1 + \frac{\Delta n_{OC}}{n_0}\right) + \frac{A_B}{A_{SC}}\frac{S_{SC}}{d}\right]^{-1}. \qquad (24)$$

Fig. 6a shows the calculated efficiency η dependence on the base doping level n_0. As can be seen from the figure, the maximum of $\eta(n_0)$ = 21.69% is reached at $n_0 = 5.5 \cdot 10^{15}$ cm^{-3}, this differs from the experimental value by less than one percent.

Using the expression (19), the coefficient *b* from the phenomenological formula (21) for *EQE*(λ) in the long-wave range can be found, and it equals to 4. Using $b = 4$, as well as the expression (20) for the short-circuit current dependent on the base thickness *d*, we can calculate the base thickness dependent photoconversion efficiency, which is shown in Fig. 6b. As can be seen from the figure, the maximum η = 21.72% is reached at d = 750 μm, which is only one percent higher than the experimental value.

The comparison of experimental and theoretical results in Figs 2, 4 and 6 clearly demonstrates a very good agreement and proves that the developed formalism can be successfully used not to only better understanding the photoconversion mechanisms and its limiting factors in a wide class of the highly-efficient silicon-based textured SCs. More important is that this enables to optimize SCs in terms of their parameters.

5. Conclusions

This work generalizes and refines the analytical approach that we proposed and used earlier to analyze high-efficiency solar cells and modeling of their main characteristics.

We have experimentally characterized the high efficiency commercial SunPower™ IBC SCs, including measurements of the photocurrent density dependence $J_L(V_{OC})$ on the open-circuit voltage V_{OC} in a wide range of the V_{OC} values, which allows finding the more correct dependence of the total effective recombination lifetime $\tau_{eff}(\Delta n)$ on the excess carrier concentration Δn. The measurements demonstrate that at $\Delta n < 4 \cdot 10^{14}$ cm^{-3} the lifetime τ_{eff} decreases with decreasing Δn, which indicates a significant effect of recombination in SCR in the area with the excess concentrations of electron-hole pairs. This is also evidenced by the dark *I–V* characteristics of SCs under consideration. It has been ascertained that the dependences of the short-circuit current on the open-circuit voltage and the dark current on the applied voltage at $V < 0.62$ V coincide with each other.

To reproduce the experimental results theoretically, we proposed the comprehensive and physically transparent analytical formalism to model and optimize the high efficiency textured silicon-based solar cells. Its application proves that the contribution of nonradiative exciton recombination by the Auger mechanism *via* deep recombination centers, as a rule, exceeds the radiative recombination contribution and substantially affects the photoconversion efficiency, stronger than the effect of bandgap narrowing.

The developed approach allows us to correctly model the short-circuit current and the efficiency of photoconversion in the highly efficient textured silicon solar cells. The proposed formalism allows one to self-consistently calculate such key SCs parameters as the short-circuit current density J_{SC}, open-circuit voltage V_{OC} and photoconversion efficiency η on the doping level and base thickness. These calculations have been carried out for several SCs types to achieve very good agreement of the calculated characteristics with the experimental ones. This allows also to optimize the base thickness technologically important for SCs and the doping level. It has been also shown that the recombination in SCR decreases the effective recombination time $\tau_{eff}(\Delta n)$ in the region of small Δn values.

Our analysis enables to conclude that the standard experimentally measured SCs characteristics, namely: the open-circuit voltage V_{OC}, short-circuit current density J_{SC}, fill factor *FF*, as well as the power P_m, voltage V_m, current density J_m at the maximum power point, junction saturation current density J_0, are usually not sufficient to comprehensively model and optimize the textured silicon SCs. To carry out this modeling and optimization, the experimental dependence $\tau_{eff}(\Delta n)$ measured using the ready-made SCs or the experimental $J_L(V_{OC})$ or dark *I–V* dependences are also required.

Acknowledgement

This work was partially supported (V.P. Kostylyov, V.M. Vlasiuk, R.M. Korkishko and O.Ya. Olikh) by National Research Foundation of Ukraine *via* the state budget financing (project 2020.02/0036 “Development of physical base of both acoustically controlled modification and machine learning–oriented characterization for silicon solar cells”).

References

1. Fraunhofer Institute for Solar Energy Systems. *Photovoltaics Report.* 2021. *https://www.ise.fraunhofer.de/content/dam/ise/de/documents/publications/studies/Photovoltaics-Report.pdf*.
2. Liu J., Yao Y., Xiao S., and Gu X. Review of status developments of high-efficiency crystalline silicon solar cells. *J. Phys. D.* 2018. **51**. P. 123001. https://doi.org/10.1088/1361-6463/aaac6d.
3. Green M., Dunlop E., Hohl-Ebinger J. *et al*. Solar cell efficiency tables (Version 58). *Prog. Photovoltaics: Res. Appl*. 2021. **29**, Issue 7. P. 657–667. https//doi.org/10.1002/pip.3444.
4. Yoshikawa K., Kawasaki H., Yoshida W. *et al*. Silicon heterojunction solar cell with interdigitated back contacts for a photoconversion efficiency over 26%. *Nature Energy.* 2017. **2**. P. 17032. https://doi.org/ 10.1038/nenergy.2017.32.
5. Sachenko A., Kostylyov V., Sokolovskyi I., and Evstigneev M. Effect of temperature on limit photoconversion efficiency in silicon solar cells. *IEEE Journal of Photovoltaics*. 2020. **10**. P. 1–7. https://doi.org/10.1109/JPHOTOV.2019.2949418.
6. Yoshikawa K., Yoshida W., Irie T. *et al*. Exceeding conversion efficiency of 26% by heterojunction

interdigitated back contact solar cell with thin film Si technology. *Solar Energy Mater. Solar Cells.* 2017. **173**. P. 37–42. https://doi.org/10.1016/J.SOLMAT.2017.06.024.
7. Augusto A., Karas J., Balaji P., Bowden S.G., and King R.R. Exploring the practical efficiency limit of silicon solar cells using thin solar-grade substrates. *Mater J. Chem. A.* 2020. **8**. P. 16599. https://doi.org/10.1039/D0TA04575F.
8. Sachenko A.V., Kostylyov V.P., Vlasiuk V.M., Sokolovskyi I.O., and Evstigneev M. Influence of excitonic effects on luminescence quantum yield in silicon. *J. Lumin.* 2017. **183**. P. 299–302. https://doi.org/10.1016/j.jlumin.2016.11.028.
9. Sachenko A.V., Kostylyov V.P., Vlasiuk V.M. *et al*. Features in the formation of a recombination current in the space charge region of silicon solar cells. *Ukr. J. Phys.* 2016. **61**. P. 917–922. https://doi.org/10.15407/ujpe61.10.0917.
10. See, e.g., https://www.pvlighthouse.com.au/simulation-programs for the solar cell simulation software.
11. Sachenko A., Kostylyov V., Sokolovskyi I. *et al.* Limit temperature coefficient in silicon solar cells. *47th IEEE Photovoltaic Specialists Conference (PVSC)*. 2020. P. 0715. https://doi.org/10.1109/PVSC45281.2020.9300383.
12. Sachenko A.V., Kostylyov V.P., Bobyl A.V. *et al*. The effect of base thickness on photoconversion efficiency in textured silicon-based solar cells. *Techn. Phys. Lett.* 2018. **44**. P. 873–876. https://doi.org/10.1134/S1063785018100139.
13. Green M.A. Lambertian light trapping in textured solar cells and light-emitting diodes: Analytical solutions. *Prog. Photovoltaics: Res. Appl.* 2002. **10**. P. 235–241. https://doi.org/10.1002/pip.404.
14. Sachenko A.V., Kryuchenko Y.V., Kostylyov V.P. *et al*. Temperature dependence of photoconversion efficiency in silicon heterojunction solar cells: Theory *vs* experiment. *J. Appl. Phys*. 2016. **119**. P. 225702. https://doi.org/10.1063/1.4953384.
15. Sachenko A., Kostylyov V., Vlasiuk V., Sokolovskyi I., and Evstigneev M. Optimization of textured silicon solar cells. *47th IEEE Photovoltaic Specialists Conference (PVSC)*. 2020. P. 0719. https://doi.org/10.1109/PVSC45281.2020.9300877.
16. Tiedje T., Yablonovitch E., Cody G.D., and Brooks B.G. Limiting efficiency of silicon solar cells. *IEEE Trans. Electron Devices.* 1984. **31**. P. 711. https://doi.org/10.1109/T-ED.1984.21594.
17. Niewelt T., Richter A., Kho T.C. *et al.* Taking mono-crystalline silicon to the ultimate lifetime limit. *Solar Energy Mater. Solar Cells.* 2018. **185**. P. 252–259. https://doi.org/10.1016/j.solmat.2018.05.040.
18. Richter A., Glunz S.W., Werner F. *et al*. Improved quantitative description of Auger recombination in crystalline silicon. *Phys. Rev. B.* 2012. **86** P. 165202. https://doi.org/10.1103/PhysRevB.86.165202.
19. Gorban A.P., Kostylyov V.P., Sachenko A.V., Serba A.A., and Sokolovsky I.O. Impact of excess charge carrier concentration on effective surface recombination velocity in silicon photovoltaic structures. *Ukr. J. Phys.* 2006. **51**. P. 598.
20. Sachenko A.V., Kostylyov V.P., Sokolovskyi I.O. *et al*. Specific features of current flow in α-Si:H/Si heterojunction solar cells. *Techn. Phys. Lett*. 2017. **43**. P. 152–155. https://doi.org/10.1134/S1063785017020109.
21. Sah C., Noyce R.N., and Shockley W. Carrier generation and recombination in *p-n* junctions and *p-n* junction characteristics. *Proc. IRE*. 1957. **45**. P. 1228. https://doi.org/10.1109/JRPROC.1957.278528.
22. Sproul A.B. and Green M.A. Intrinsic carrier concentration and minority carrier mobility of silicon from 77 to 300 K. *J. Appl. Phys.* 1993. **73**. P. 1214. https://doi.org/10.1063/1.353288.
23. Smith D.D., Reich G., Baldrias M., Reich M., Boitnott N., and Bunea G. Silicon solar cells with total area efficiency above 25%. *43rd IEEE Photovoltaic Specialists Conference (PVSC)*. 2016. P. 3351–3355. https://doi.org/10.1109/PVSC.2016.7750287.

Authors and CV

Sachenko A.V. Professor, Doctor of Physical and Mathematical Sciences, Chief Researcher of the Laboratory of Physical and Technical Fundamentals of Photovoltaics at the V. Lashkaryov Semiconductor Institute of Semiconductor Physics. He is the author of more than 300 scientific publications. His main research interests include analysis, characterization, and modeling of silicon solar cells.
E-mail: sach@isp.kiev.ua,
https://orcid.org/0000-0003-0170-7625

Kostylyov V.P. Professor, Doctor of Physical and Mathematical Sciences, Head of the Laboratory of Physical and Technical Fundamentals of Semiconductor Photovoltaics at the V. Lashkaryov Institute of Semiconductor Physics. He is the author of more than 250 scientific publications. The area of his scientific interests includes development of equipment for silicon solar cells testing, research, analysis of silicon solar cells.
E-mail: vkost@isp.kiev.ua,
https://orcid.org/0000-0002-1800-9471

Korkishko R.M. PhD, Researcher of the Laboratory of Physical and Technical Fundamentals of Semiconductor Photovoltaics, V. Lashkaryov Institute of Semiconductor Physics. He is the author of more than 46 scientific publications. The area of his scientific interests includes research, analysis of silicon solar cells.
E-mail: romkin.ua@gmail.com;
https://orcid.org/0000-0002-4568-574X

Vlasiuk V.M. PhD, Researcher of the Laboratory of Physical and Technical Fundamentals of Semiconductor Photovoltaics at the V. Lashkaryov Institute of Semiconductor Physics. He is the author of more than 47 scientific publications. The area of his scientific interests includes research and analysis of silicon solar cells. E-mail: viktorvlasiuk@gmail.com,
https://orcid.org/0000-0001-6352-0423

Sokolovskyi I.O. PhD, Senior Researcher of the Laboratory of Physical and Technical Fundamentals of Semiconductor Photovoltaics at the V. Lashkaryov Institute of Semiconductor Physics. He is the author of more than 70 scientific publications. His main research interests include modeling of silicon solar cells.
E-mail: falcon128@gmail.com,
https://orcid.org/0000-0002-7072-6670

Evstigneev M.A. Assistant Professor of the faculty of Physics and Physical Oceanography at the Memorial University of Newfoundland. His research areas are non-equilibrium statistical physics, biophysics, surface sciences.
E-mail: mevstigneev@mun.ca,
https://orcid.org/0000-0002-7056-2573

Olikh O.Ya. Doctor of Physical and Mathematical Sciences of the faculty of Physics at the Taras Shevchenko National University. His research areas include the effect of ultrasound on the substance, acoustic-stimulated dynamic phenomena in semiconductor barrier structures.
E-mail: olegolikh@knu.ua,
https://orcid.org/0000-0003-0633-5429

Shkrebtii A.I. Professor at the Ontario Tech University. His recent focus is on hydrogen-bonding, nanomaterials hydrogenation, ubiquitous in physical, chemical and biological sciences.

E-mail: Anatoli.Chkrebtii@ontariotechu.ca
https://orcid.org/0000-0002-4998-1538

Dvernikov B.F. Researcher of the Laboratory of Physical and Technical Fundamentals of Semiconductor Photovoltaics at the V. Lashkaryov Institute of Semiconductor Physics. The area of his scientific interests includes manufacturing the equipment for silicon solar cells testing.
E-mail: dvernikov@isp.kiev.ua;
https://orcid.org/0000-0003-2917-8948

Chernenko V.V. Senior Researcher of the Laboratory of Physical and Technical Fundamentals of Semiconductor Photovoltaics, V. Lashkaryov Institute of Semiconductor Physics. He is the author of more than 100 scientific publications. His main research interests include research and analysis of silicon solar cells.
E-mail: vvch@isp.kiev.ua,
https://orcid.org/0000-0002-7630-6925

Authors' contributions

Sachenko A.V.: conceptualization, formal analysis, theoretical investigations, writing – original draft, editing.
Kostylyov V.P.: conceptualization, formal analysis, validation, writing – review & editing, project administration.
Korkishko R.M.: experiment preparation, experimental investigation, editing.
Vlasiuk V.M.: experimental investigation, preparation of experimental data, visualization, editing.
Sokolovskyi I.O.: visualization, theoretical investigations, editing.
Evstigneev M.: theoretical investigations, editing.
Olikh O.Ya.: literary research, editing.
Shkrebtii A.I.: theoretical investigations, editing.
Dvernikov B.F.: experiment preparation, editing.
Chernenko V.V.: literary research, editing.

Експериментальне дослідження та теоретичне моделювання текстурованих кремнієвих сонячних елементів із тильною металізацією

А.В. Саченко, В.П. Костильов, Р.М. Коркішко, В.М. Власюк, І.О. Соколовський, М. Євстигнєєв, О.Я. Оліх, А.І. Шкребтій, Б.Ф. Дверников, В.В. Черненко

Анотація. Кристалічний кремній (c-Si) залишається домінуючим фотоелектричним матеріалом у промисловості сонячних батарей. На даний час науково-технічний прогрес дозволяє виробляти c-Si сонячні елементи (СЕ) з ефективністю, близькою до фундаментальної межі. Тому поєднання експериментальних результатів і результатів моделювання стає вирішальним для подальшого прогресу у підвищенні ефективності та зниженні вартості фотоелектричних систем. Проведено експериментальну характеристику високоефективних c-Si СЕ та порівняно з результатами моделювання. Для цього ми розробили та застосували до досліджуваних зразків удосконалену теоретичну модель для оптимізації характеристик високоефективних текстурованих сонячних елементів. Модель враховує всі механізми рекомбінації, включаючи безвипромінювальну рекомбінацію екситонів за Оже-механізмом через глибокі центри рекомбінації та рекомбінацію в області просторового заряду. Для порівняння теоретичних результатів із експериментальними нами запропоновано емпіричну формулу зовнішньої квантової ефективності, яка описує її експериментальну спектральну залежність поблизу довгохвильового краю поглинання. Запропонований підхід дозволяє моделювати струм короткого замикання та ефективність фотоперетворення у сонячних елементах текстурованого кристалічного кремнію. Установлено, що залежності струму короткого замикання від напруги холостого ходу та темнового струму від прикладеної напруги при $V < 0{,}6$ В збігаються. Теоретичні результати у порівнянні з експериментальними дозволили підтвердити розроблений формалізм і були використані для оптимізації основних параметрів СЕ, таких як товщина основи, рівень легування та ін. У цій роботі ми додатково узагальнили та вдосконалили аналітичний підхід, запропонований і використаний нами раніше для аналізу високоефективних сонячних елементів і моделювання їх характеристик.

Ключові слова: кремній, сонячний елемент, текстура, ефективність, рекомбінація, оптимізація.